Myelin biogenesis

Ozgen, Hande

Chapter 3

The major myelin-resident protein PLP is transported to myelin membranes via a transcytotic mechanism: Involvement of sulfatide

Wia Baron[1], Hande Ozgen[1]*, Bert Klunder[1]*, Jenny C. de Jonge[1], Anita Nomden[1], Annechien Plat[1], Elisabeth Trifilieff[2], Hans de Vries[1] and Dick Hoekstra[1]

[1] Department of Cell Biology, University of Groningen, University Medical Center Groningen, Antonius Deusinglaan 1, 9713 AV Groningen, the Netherlands
[2] UMR_S U1119 INSERM / Université de Strasbourg, Faculté de Médecine, 4 rue Kirschleger, 67085 Strasbourg, France
**equal contribution*

Manuscript Under Revision

Abstract

Myelin membranes are sheet-like extensions of oligodendrocytes that can be considered as membrane domains distinct from the cell's plasma membrane, consisting of myelin-specific proteins and lipids. Previous data suggest that myelin membrane-directed trafficking displays typical basolateral features. Consistent with the polarized nature of oligodendrocytes we demonstrate here that transcytotic transport of the major myelin-resident protein, PLP, is a key element in the mechanism of myelin assembly. Upon biosynthesis, PLP traffics to myelin membranes via syntaxin 3-mediated docking at the apical membrane-like cell body plasma membrane, which is followed by subsequent internalization and transport to the myelin sheet. A similar transcytotic transport from apical to basolateral membrane domain is observed, when PLP is expressed in polarized HepG2 cells. In both cell types, PLP dynamically partitions into different lateral membrane pools, characterized by insolubility in the non-ionic detergents TX-100 or CHAPS. Pulse chase experiments, in conjunction with surface biotinylation and organelle fractionation, reveal that following biosynthesis, PLP is transported to the cell body surface in TX-100-resistant microdomains. At the plasma membrane, PLP transiently resides within these microdomains, and its lateral dissipation is followed by segregation into CHAPS-resistant domains, internalization and transport towards myelin membranes. Sulfatide triggers PLP's reallocation from TX-100- into CHAPS-resistant membrane domains, while inhibition of sulfatide biosynthesis inhibits transcytotic PLP transport. Taken together, we propose a model in which PLP transport to the myelin membrane proceeds via a transcytotic mechanism, mediated by sulfatide, and characterized by a conformational alteration and a dynamic, i.e., transient partitioning of PLP into distinct membrane domains, involved in biosynthetic and transcytotic transport, respectively.

1. Introduction

Oligodendrocytes (OLGs) synthesize a multilamellar membrane structure, known as the myelin sheath (in vitro: myelin sheet), which extends from their plasma membrane and wraps around axons, thereby facilitating rapid saltatory conduction and axonal survival in the central nervous system (CNS). Myelin is enriched in glycosphingolipids and cholesterol, and contains myelin-specific proteins of which myelin basic protein (MBP) and proteolipid protein (PLP) are the major ones [1,2]. In generating a myelin membrane, OLGs acquire a polarized phenotype, whereby the myelin membrane is served by a 'basolateral-like' and the cell body plasma membrane by an 'apical-like' transport mechanism [3–7]. MBP and PLP stabilize

apposed myelin membrane surfaces in compact myelin, and their transport routes are segregated. Thus, following its biosynthesis at the rough endoplasmic reticulum(RER) and processing through the Golgi apparatus [8,9], the transmembrane protein PLP is transported via vesicles to the myelin membrane [10,11]. In marked contrast, MBP, a peripheral membrane protein facing the cytoplasm, is synthesized at and associates with the myelin membrane 'on site', involving myelin membrane-directed transport of its mRNA rather than the native protein [12]. In addition, to limit ectopic assembly and premature compaction of myelin membranes, the protein-mediated biogenesis of myelin membranes is tightly regulated, both in time and space (reviewed in [5]). In fact, MBP associates with myelin membranes prior to PLP [2]. Regulation of trafficking of either protein is under tight neuronal control, MBP trafficking being mainly regulated by adhesive interactions [13,14], while the flow of PLP appears to be governed by secreted factors [15]. Clearly, defining the processes of cellular sorting and transport, in which lipid-protein interactions with environmental signals regulate OLG development, is essential for an understanding of both normal OLG development and the process of remyelination in demyelinating diseases such as multiple sclerosis (MS), in which the myelin membrane organization is perturbed.

The underlying sorting machinery as to how PLP reaches its final destination is still unclear, but insight into the overall transport pathway is gradually emerging and favors indirect transport of PLP to myelin membranes in OLGs. Thus prior to reaching the myelin membrane, evidence suggests that PLP is sorted to and stored in a late LAMP1-positive endosomal compartment [10,15,16], from where the protein, along with cholesterol, and in galactosylceramide (GalC)-enriched microdomains, is subsequently transported to the myelin membrane, triggered by a neuronal-derived soluble cAMP-dependent mechanism [15]. To reach this late endosomal compartment, PLP is internalized from the plasma membrane via clathrin-independent but cholesterol-dependent endocytosis [15–17]. Recently, delivery of PLP to the surface has been claimed to occur by two independent pathways, involving the v-SNAREs VAMP3 and VAMP7, respectively [18]. Therefore, in line with the presence of polarity-based transport mechanisms in OLGs, newly synthesized PLP might reach its final destination via an indirect, transcytotic pathway. Consistent with this hypothesis is the observation that PLP, stably expressed in polarized Madin-Darby canine kidney (MDCK) cells, is transported to the apical rather than basolateral surface [19], i.e., membrane domains bearing reminiscence to the cell body plasma membrane and the myelin-like membrane in cultured OLGs, respectively [3,4].

Thus far knowledge concerning docking and final insertion of PLP into the myelin membrane is scanty. A variety of syntaxins, i.e., t-SNAREs involved in the docking and fusion of transport vesicles at target membranes, has been detected in OLGs [5,20,21],

including syntaxins 3 and 4, the respective putative binding partners of VAMP7 and VAMP3 [18,21]. Specifically, in previous work we have shown a polarized distribution of these syntaxins, syntaxin 3 localizing largely at the plasma membrane of the OLG cell body and the primary processes, whereas syntaxin 4 is enriched at the myelin sheet [5]. To obtain further insight into the molecular mechanism underlying PLP trafficking and its assembly into the myelin sheath the current study was undertaken. Our data demonstrate that PLP is transported to myelin membranes via a transcytotic route, involving syntaxin 3, localized at the OLG cell body plasma membrane, followed by a sulfatide-facilitated shift into a different lateral membrane pool which is accompanied by conformational alterations, prior to the protein's delivery to the myelin sheet.

2. Materials and Methods

2.1. Cell cultures

Oligodendrocytes (OLGs). Primary cultures of OLGs were prepared from forebrains of 1-2 day old Wistar rats as described previously [22,23]. Oligodendrocyte progenitor cells (OPCs) were plated in SATO supplemented with the growth factors FGF-2 (10 ng/ml, Peprotech, London, UK) and PDGF-AA (10 ng/ml, Peprotech) on poly-L-lysine (PLL, 5 µg/ml, Sigma, St. Louis, MO)-coated 10 cm dishes (Nunc, Naperville, IL,1.0 106 cells/dish) or 8-well permanox chamber slides (Nunc, 20,000 cells/well), for biochemical and immunocytochemical analysis, respectively. After 2 days ('OPCs'), differentiation was initiated by switching to SATO supplemented with 0.5% fetal calf serum (FCS, Bodinco, Alkmaar, the Netherlands), and cells were grown for 3 days (imOLGs) or 7-10 days (mOLGs). To inhibit sulfatide biosynthesis, cells were cultured in the presence of 30 µM sodium chlorate for at least 4-7 days.

OLN-PLP cells. OLN-PLP cells were made in the laboratory of Dr. Zeger Debyser (University of Leuven, Belgium) in collaboration with Dr. Rik Gijsbers and Veerle Baekelandt (University of Leuven, Belgium) and were a kind gift of Dr. Ellen Gielen (Hasselt University, Belgium). Briefly, PLP was cloned into the lentiviral plasmid pCOMBI-eGFP-IRES-puro, and PLP-eGFP containing lentiviral particles were produced using HEK-293T cells. Subsequently, the rat-derived oligodendroglia derived cell line, OLN-93, a kind gift of Dr. Christiane Richter Landsberg (University of Oldenburg, Germany, [24]) was lentivirally transduced with the PLP-eGFP containing lentiviral particles. OLN-PLP cells were cultured in DMEM containing 10% heat-inactivated FCS, and in the presence of 2 µg/ml puromycin (Sigma). Cells were plated on 8-well permanox chamber slides for immunocytochemistry (5,000 cells/well) or on 10 cm

tissue culture dishes for biochemical analysis (500,000 cells/well). Cells were grown in DMEM supplemented with 10% FCS for 3 days, unless otherwise indicated.

HepG2 cells. HepG2 cells were cultured in DMEM containing 10% FCS. Transfection of HepG2 cells with the plasmid pLEGFP-N1-PLP was performed with Lipofectamin 2000 (Invitrogen, Breda, The Netherlands), according to the manufacturer's instructions. After transfection, the cells were cultured in the presence of 1.0 mg/ml geneticin (G418, Invitrogen), and colonies were isolated 14 days after transfection. Stably transfected cells were plated on 8-well permanox chamber slides for immunocytochemistry (5,000 cells/well) and on 10 cm tissue culture dishes for biochemical analysis (500,000 cells/well).

2.2. Constructs

The cDNA encoding syntaxin 3 and PLP-eGFP were a kind gift of Drs. Thomas Weimbs (University of California Santa Barbara, CA, [25]), and Niels Hellings (Hasselt University, Belgium). For cloning of the syntaxin 3 gene into the retroviral vector pLXIN (Clontech Biosciences, Mountain View, CA), a XhoI restriction site at the ATG start codon and a XhoI restriction site after the stop codon were introduced by PCR. The following primers were used: 5'CATGTATTCGAAGAGCTCTTCGCACATG 3' (forward syntaxin 3), 5'CTAGGTGATCAAGAGCTCCTAGGGCCCACG 3' (reverse syntaxin 3). The cDNAs encoding ceramide sulfatide transferase (CST) and ceramide galactosyltransferase (CGT) were kind gifts of Drs. Matthias Eckhardt (University of Bonn, Germany) and Brian Popko (University of Chicago, IL), respectively. For cloning, the cst and cgt genes were inserted into the EcoRI site of the retroviral vector pLXIN (Clontech Biosciences, Mountain View, CA). The orientation and the integrity of the obtained pLXIN constructs were confirmed by DNA sequencing.

2.3. Retroviral transduction

The production of retroviral particles and the subsequent infection of OPCs and OLN-PLP cells were performed according to Klunder et al. [3], and Maier et al., [26], respectively Transductions were carried out by exposing cells to retroviral particles and 8 μg/ml hexadimethrine bromide (polybrene, Sigma), for 16-18 hrs. The cells werecultured for 24 hrs and then cultured under selection at proliferating conditions in the presence of 400 μg/ml (OPCs) or 2 mg/ml (OLN-PLP-cells) G418 (Roche, Mannheim, Germany) during 5 days. OLN-PLP cells were first infected with CGT (OLN-PLP-G), and subsequently selected, which was followed by a second infection with CST(OLN-PLP-GS). An OLN-MOCK cell line was obtained by retroviral infection with

vector-only (pLXIN). The transduction efficiency was nearly 100%. OLN-PLP-G and OLN-PLP-GS cells were cultured in the presence of 2 µg/ml puromycin and 2 mg/ml G418 (Roche).

2.4. PLP antibodies

PLP consists of four hydrophobic α-helices that span the lipid bilayer with two extracytoplasmic domains and three cytoplasmic domains, while both the C- and N terminus face the cytoplasm [27,28]. The anti-PLP antibodies 4C2, directed against a non-conformational epitope in the first extracellular loop (PLP 50-69), and 2D2, directed against an intracellular region absent in DM-20 (PLP 100-123), were kind gifts of Dr. Vijay Kuchroo (Harvard Medical School, Boston, [29]). The epitope recognized by the anti-PLP antibody O10 is acquired posttranslational and is directed against a conformational dependent epitope in the second extracellular loop [kind gift of Dr. Evi Albers-Krämer (Mainz, Germany,[30])]. The anti-PLP antibody ET3 was raised in rabbits against the second extracellular loop of PLP. To this end a synthetic peptide, PLP181-230, with the two disulfide bridges was generated [31]. Two rabbits were injected subcutaneously on days 0, 21, 35 with an emulsion containing 300 mg of this synthetic peptide in either Freund's complete adjuvant (day 0) or incomplete adjuvant (days 21 and 35). At day 49, 600 mg of the peptide in incomplete adjuvant was injected. The rabbits were bled on day 56 and the serum were kept frozen at - 20° C. The ET3 antibody reacts with the peptide in an ELISA and recognizes a conformational epitope, given the absence of a band in reducing Western blots (data not shown).

2.5. Pulse-chase experiment

Immature OLGs were pre-incubated in DMEM without methionine (Invitrogen, Breda, The Netherlands) for 1 hr, followed by a 10 min labeling with µ200 Ci/dish Tran35S-label (GE Healthcare, BioSciences, Buckinghamshire, UK). The cells were then 'chased' with medium supplemented with 10 mM methionine (Merck, Darmstadt, Germany) for 0, 15, 30 and 60 min. Cells were scraped in phosphate buffered saline (PBS), extracted with TNE-lysis buffer [20 mM Tris-HCl pH 7.4, 150 mM NaCl, 1 mM EDTA supplemented with 1% Triton X-100 (TX-100) and a cocktail of protease inhibitors (Complete Mini, Roche)] for 30 min at 4°C, and separated by centrifugation (15 min at 13,300 g) into TX-100-soluble supernatants and TX-100-insoluble pellets. PLP was immunoprecipitated from both fractions with protein G-sepharose (GE Healthcare) beads overnight at 4°C. Protein G-sepharose beads were washed four times with TNE-lysis buffer supplemented with 0.2% SDS and once with PBS. Washed

protein G-sepharose beads were resuspended in SDS sample buffer, and counted for 2 min in a microplate scintillation and luminescence counter (Packard Instrument Company, Meriden, CT).

2.6. Preparation of detergent extracts

Cells were washed with PBS, and harvested by scraping the cells in TNE-lysis buffer containing either 1% TX-100 or 20 mM 3-[(3-cholamidopropyl)dimethylammonio]-2-hydroxy-1-propanesulfonate (CHAPS). The solution was passed 10 times through a 21-gauge needle and incubated on ice for at least 30 min. The protein content was determined by a Bio-Rad DC Protein Assay (Bio-Rad Laboratories, Hercules, CA), using bovine serum albumin (BSA) as a standard.

2.7. OptiPrep density gradient centrifugation

For density gradient centrifugation a discontinuous OptiPrep gradient was prepared. To this end, 250 µl of total cell detergent extracts (equal protein) were added to 500 µl of 60% OptiPrep. This 40% OptiPrep solution was overlaid with 30% and 10% OptiPrep. Gradients were centrifuged overnight at 152,000 g (SW55 Beckman, 4°C) and seven gradient fractions were collected from the top (fraction 1) to the bottom (fraction 7). To concentrate proteins, equal fraction volumes were adjusted to a final volume of 1 ml with TNE-buffer and treated with deoxycholate (125 µg/ml) for 5 min at 4°C followed by precipitation with 6.5% trichloric acid (TCA) for 15 min at 4°C. Precipitates were centrifuged for 20 min at 9,200 g and 4°C. The pellets were dried and resuspended in SDS-reducing sample buffer. After the pH was adjusted to 6.8 by exposure to ammonia, the samples were heated for 30 min at 37°C and subjected to SDS PAGE and Western blotting.

2.8. Surface biotinylation

Cells were washed twice with ice-cold PBS, and incubated for 1 hr with Sulfo-NHS-L-C-Biotin (0.1 mg/ml in PBS, Pierce, Rockford, IL) at 4°C. The cells were washed three times for 5 min with cell wash buffer (CWB, 65 mM Tris-HCl pH 7.5, 150 mM NaCl, 1 mM CaCl2, 1 mM MgCl2) to remove excess biotin and twice with PBS. The cells were harvested by scraping in 350 µl TNE-lysis buffer and pressed 18 times through a 21-gauge needle. Lysis occurred on ice for 30 min and the protein content was determined by the Bio-Rad DC Protein Assay. Equal amounts of protein were centrifuged for 20 min at 15,600 g to obtain soluble and insoluble fractions, or

subjected to OptiPrep density gradient centrifugation. Biotinylated proteins from equal volumes of the fractions were immunoprecipitated with streptavidin (SA)-agarose for 16-18 hrs at 4°C. After centrifugation, the SA-agarose beads (biotinylated proteins) were washed four times with CWB supplemented with 1% NP-40 and 0.35 M NaCl and once with PBS. Non-biotinylated proteins (supernatants) were concentrated by TCA precipitation (see above). Samples from SA-agarose beads (surface) and supernatant (intracellular) fractions were mixed with SDS reducing sample buffer, heated for 2 min at 95°C or 30 min at 37°C and subjected to SDS-PAGE and Western blotting.

2.9. Isolation of endosomes and lysosomes

Endosomal and lysosomal enriched fractions were isolated from cells by the flotation-gradient fractionation method [32,33]. Cells were harvested by scraping into 250 mM sucrose, 20 mM HEPES and 0.5 mM EGTA at pH 7.0 (homogenization buffer, HB) and immediately subjected to the isolation procedure. Cells were washed twice with HB by centrifugation at 800 g for 5 min at 4oC. The pellet was resuspended in 1 ml of HB supplemented with protease inhibitors and homogenized with a grounding glass cell douncer (15x loose and 10x tight). The homogenate was centrifuged at 800 g for 10 min at 4°C. The obtained post-nuclear supernatant was centrifuged at 15,000 g for 15 min at 4°C, to remove mitochondria. Subsequent centrifuging of the supernatant at 128,000 g for 1 hr at 4°C removed the microsomal fraction. The remaining endosomal and lysosomal enriched fractions were separated from each other on a discontinuous sucrose density gradient. To this end, the pellet was resuspended in 1 ml 40.6% sucrose solution and passed 10 times through a 25 gauge needle. The 40.6% sucrose/protein mixture was overlaid sequentially with sucrose solutions of 35% (1.5 ml), 30% (1.5 ml), 25% (2 ml) and HB (6 ml). The gradient was centrifuged at 125,000 g for 2 hrs at 4oC (SW41-Ti rotor). Fractions of 1 ml were collected from the top (fraction 1) to the bottom (fraction 12). The fractions were diluted with 2 ml of 20 mM HEPES and 0.5 mM EGTA at pH 7.0 and centrifuged at 153,000 g for 30 min at 4°C (TLA 100.3 rotor). Pellets were resuspended in 160 µl TNE, passed 5 times through a 25G needle and stored at -20oC. Of note, the pellets of fractions 1-4 were pooled.

2.10. Analysis of cellular glycosphingolipids

Cells were washed three times with PBS, harvested by scraping in PBS, centrifuged at 9,200 g at room temperature (RT), followed by lipid extraction of the cell pellet

according to Bligh and Dyer [34]. Lipids were separated on TLC plates using C3H6O2/ CH3CH(OH)CH3/CHCl3/CH3OH/25% KCl (25:25:25:10:9, v/v/v/v/v) as the running solvent. To visualize the glycosphingolipids, the plates were dried, and sprayed with 10% H2SO4 and 5% CH3OH and heated to 120°C.

2.11. Immunocytochemistry and in situ extraction

Antibody staining of cell surface components were performed on living cells at 4°C. After blocking non-specific binding with 4% BSA in PBS, cells were incubated with the anti-surface PLP antibodies 4C2 (1:5), ET3 (1:50), and O10 (1:3), or anti-sulfatide antibody O4 or anti-GalC antibody O1 (1:1 and 1:10, respectively, kind gifts of Dr. Guus Wolswijk, [35]) for 30 min, washed three times and incubated for 25 min with appropriate FITC- or TRITC-conjugated secondary antibodies (Jackson ImmunoResearch, West Grove, PA). The cells were fixed with 4% paraformaldehyde (PFA, Merck) in PBS for 20 min at RT. For double or single staining of intracellular antigens, PFA-fixed cells were permeabilized and blocked with 0.1 % TX-100 and 4% BSA, respectively, in PBS for 30 min at RT. The cells were incubated for 1-2 hrs with anti-PLP (1:5, 4C2 or 2D2), anti-MRP-2 (1:300, Axxora, Lörrach, Germany) or anti-GFP antibodies (1:100, Invitrogen, Molecular Probes, Eugene, OR) at RT. The cells were washed with PBS and incubated with appropriate FITC- or TRITC-conjugated secondary antibodies and DAPI (1 µg/ml, Sigma) for 25 min at RT. After washing with PBS, the cells were covered with 2.5% 1,4-diazobicyclo[2.2.2]octane (DABCO) in 90% glycerol/ 10% PBS, to prevent image fading. For in situ extraction, cells were exposed to cold 0.5% TX-100 or 10 mM CHAPS in PBS for 2 min at 4°C, followed by PFA-fixation at 4°C. The samples were analyzed with a conventional immunofluorescence microscope (Olympus AX70), equipped with analySIS software or with confocal microscopy using a Leica TCS SP2 or Leica SP8 AOBS Confocal Laser Scanner Microscope (Leica Heidelberg, Germany) in combination with Leica Confocal Software. Data were processed using Adobe Photoshop software.

2.12. Dotblot

Equal volumes (10 µl) of gradient fractions were applied onto nitrocellulose membranes. When dried, membranes were incubated for 1 hr at RT in blocking solution (5% nonfat dry milk in PBS), followed by an overnight incubation with the anti-sulfatide O4 antibody (ammonium sulfated precipitated, O4 1:750). After washing with PBS containing 0.1% Tween 20 (PBS-T), the membranes were incubated for 2 hrs with HRP- conjugated anti-IgM antibodies in 1% nonfat dry milk in PBS-T). Signals

were detected by enhanced chemilluminescence (ECL; GE Healthcare), scanned and quantified with Scion Image software (Scion Corp., Frederick, MD).

2.13. Antibody trafficking assay

The basolateral surface of HepG2 cells that were stably transfected with PLP-eGFP was labeled with primary antibodies diluted in 0.2% BSA in PBS for 30 min on ice, followed by a 90 min chase in culture medium at 37°C. The primary antibodies used were anti-extracellular PLP ET3 (1:5) and anti-dipeptidylpeptidase IV (DPPIV, R&D systems) antibody. The tight junctions prevent access of the antibodies to apical membrane [36]. Cells were fixed in 4% PFA for 30 min on ice, permeabilized with ice cold methanol for 10 min, blocked with 4% BSA in PBS, and incubated with the appropriate TRITC-labeled secondary antibodies. Transcytosis of the antibody-antigen complex to the apical surface was analyzed with a conventional immunofluorescence microscope (Olympus AX70), equipped with analySIS software.

2.14. SDS-PAGE and Western Blotting

Equal volume (gradient fractions) or protein amounts (cell lysates) were mixed with SDS-reducing sample buffer, heated for 5 min at 95ºC (syntaxin 3, GFP, LAMP1, EEA1) or 30 min at 37°C (PLP) and subjected to SDS-PAGE and Western blotting. Samples were loaded onto 10 or 12.5% SDS-polyacrylamide gels, transferred to Immobilon-FL (Millipore, Bedford, MA) by semi-dry blotting, and subjected to immunoblot detection as described previously [23]. Primary antibodies used were anti-syntaxin 3 (1:1000, Synaptic Systems, Göttingen, Germany), anti-PLP (1:100; 4C2), anti-GFP (1:500), anti-LAMP1 (1:250, GeneTex Inc, Irvine, CA), and anti-EEA1 (1:250, Abcam, Cambridge, UK). The signals were detected using the Odyssey Infrared Imaging System (Li-Cor Biosciences, Lincoln, NE) and analysed using Odyssey V3.0 analysis software.

2.15. Statistics

Data are expressed as mean ± standard deviation (SD) of at least three independent experiments. Statistical analysis was performed using the student t-test when two means were compared and an one sample t-test when compared relative to control, which was set to 100% in each independent experiment. When absolute values of more than two means were compared, statistical significance was calculated by one way ANOVA followed by a Tukey's post-test. In all cases a p value of $p< 0.05$ was considered significant (* $p<0.05$, ** $p< 0.01$, *** $p<0.001$).

3. Results

3.1. PLP undergoes a conformational alteration during transport to myelin membranes

The multispanning membrane protein PLP is the major myelin protein and is integrated within the specialized myelin membrane via vesicular transport. Its biosynthesis becomes distinctly apparent in immature OLGs, but rapidly increases when the cells further develop into mature myelinating cells. To accurately define its intracellular trafficking pathway following biosynthesis in a primary rat OLG monoculture system, we first determined the localization of PLP at the onset (immature OLGs) and at a more advanced stage (mature OLGs) of myelination. Examination by immunofluorescence microscopy revealed that in immature OLGs, when processes develop, PLP is abundantly localized in vesicular structures in the perinuclear region of the cell (Fig. 1A, imOLG), often showing a punctuate appearance when associated with primary processes. Furthermore, in a small subset of the cells, a prominent labeling of the plasma membrane was observed (Fig. 1A, arrow), suggesting an association of PLP with the plasma membrane of the cell body.

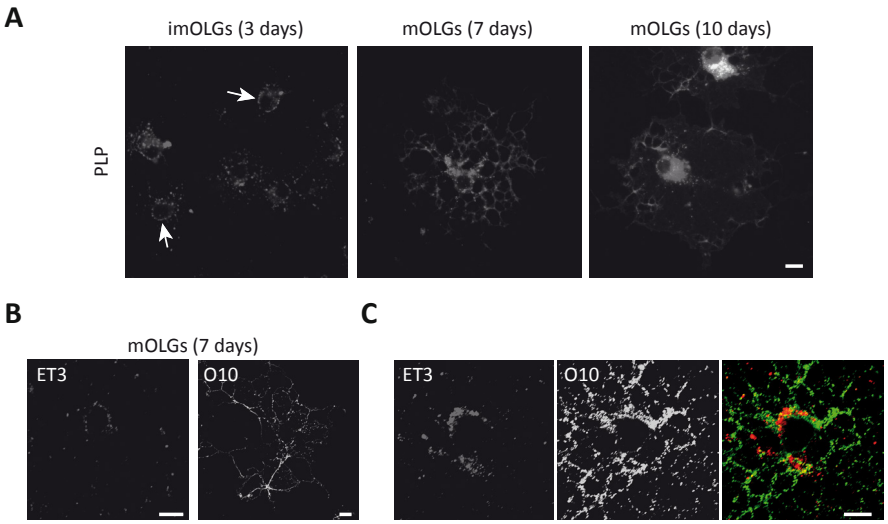

Figure 1: PLP undergoes a conformational alteration during transport to myelin membranes. A. Oligodendrocytes (OLGs) were differentiated for 3, 7 or 10 days, fixed, and permeabilized, and the localization of myelin specific protein PLP was analyzed by immunostaining (ani-PLP antibody 4C2). Note that at the immature stage (imOLG, 3 days) PLP is localized at the cell body plasma membrane (arrows), whereas in mature OLGs (mOLGs, 7 and 10 days), more PLP-containing vesicular structures in the perinuclear region in addition to myelin-sheet localization was observed. Scale bar is 10 µm. B,C. Surface staining of mature OLGs (7 days in differentiation) with PLP antibodies that recognize an extracellular epitope in the second

extracellular loop of PLP (ET3 and O10). Single labelings are shown in B; a double labeling is shown in C. Note that the ET3 antibody primarily binds to the cell body plasma membrane, whereas O10 staining is more prominent in the myelin-like membranes. Scale bar is 10 µm.

Next to its presence in the cell body, in mature, well differentiated OLGs (Fig. 1A, mOLG), the protein localizes in particular to vesicular structures in the processes and myelin-like membranes. Staining of live cells with anti-PLP ET3 antibodies (directed against a 'synthetic' second extracellular loop [31]), and O10 (directed against a conformational epitope [30]), confirmed the presence of PLP at the cell body plasma membrane and myelin-like membranes (Fig. 1B). Remarkably, although both antibodies are directed against a conformational epitope in the second extracellular loop of PLP, ET3 most prominently binds to PLP, present at the cell body plasma membrane, whereas O10 staining was more intense when PLP localized in the processes and myelin like membranes. Moreover, the staining pattern was unaltered in a double labeling, implying that these antibodies detect different epitopes (Fig. 1C). Since the secondary structure of the extracellular loop changes as a function of the environment [31], the data might indicate that during transport PLP undergoes conformational alterations and/or oligomerizes in a molecular environment-dependent manner, as reflected by differences in recognition by the conformation-specific antibodies ET3 and O10. Thus, although PLP seems to be prominently present at both cell body plasma and myelin membrane, its abundance at either membrane appears conformation-specific and apparently depends on the stage of myelin sheet development.

3.2. Overexpression of syntaxin 3 inhibits cell body plasma membrane-directed transport of PLP

In previous work, we have shown that the t-SNARE syntaxin 3, which in epithelial cells predominantly localizes at the apical plasma membrane [37,38], largely localizes at or near the plasma membrane of the OLG cell body [5], which is served by an apical-like vesicular transport route [3,4]. To assess whether PLP transport towards the myelin membrane relies on transcytosis, i.e., involves prior transport to and delivery at the cell body plasma membrane via a syntaxin 3-dependent mechanism, we examined the effect of syntaxin 3 overexpression on PLP localization. Overexpression of syntaxins leads to non-functional SNARE complexes [37], thus mimicking a dominant-negative approach. Double labeling with anti-PLP antibodies recognizing an extracellular (O10) and intracellular PLP epitope (2D2, [29]) revealed that in OLGs that overexpress syntaxin 3, transport of PLP to myelin-like membranes was apparently blocked (Fig. 2A, surface vs intracellular). Thus, at an approx. five-fold overexpression

of syntaxin 3, PLP prominently accumulated in intracellular vesicles in the cell body, without a significant appearance at either the cell surface plasma membrane or in the myelin membrane (Fig. 2A, right panels). Importantly, upon syntaxin 3 overexpression neither differences in morphology nor in the number of cells expressing MBP and PLP (data not shown) were observed, when compared to mock (vector-only)-transduced cells. Together, our data thus suggest that malfunctioning of plasma membrane-localized syntaxin 3, as a consequence of its overexpression, precludes docking of PLP-containing transport vesicles. Yet, rather than being directly transported towards the myelin membrane at such conditions, the vesicles remain trapped in the cell body cytoplasm, implying that prior docking at the cell body plasma membrane is a prerequisite for subsequent PLP transport to the myelin membrane, which presumably thus proceeds via a transcytotic mechanism.

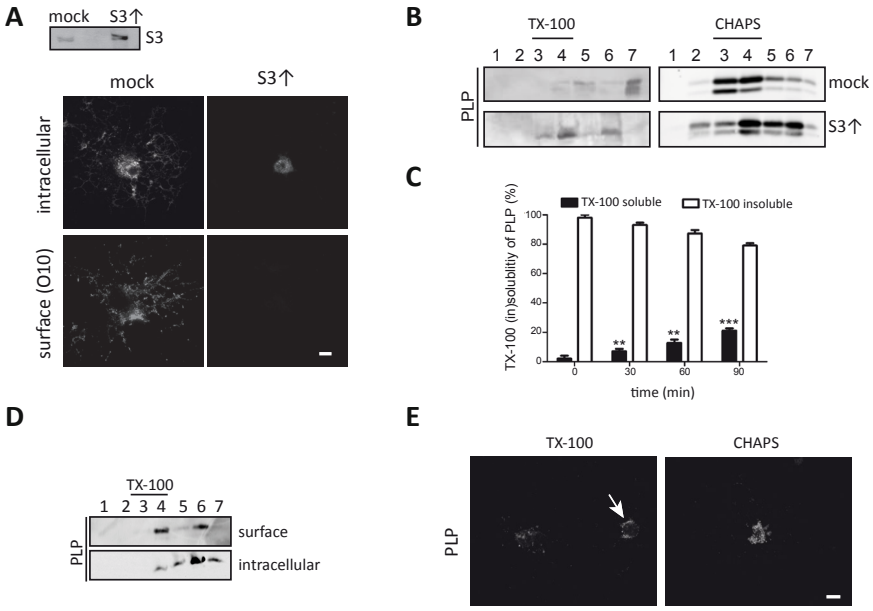

Figure 2. Overexpression of syntaxin 3 inhibits surface transport of PLP in oligodendrocytes concomitant with TX-100 resistance.

A. Oligodendrocyte progenitor cells were transduced with vector-only (mock) and syntaxin 3 (S3↑) as described in Materials and Methods. 7 days after initiating differentiation, the surface and intracellular localization of PLP was determined by immunostaining using anti-PLP antibodies directed against extracellular (O10) and intracellular PLP epitopes (2D2). Syntaxin 3 overexpression (approx. 5x) is confirmed by Western blotting. Representative pictures of three independent experiments are shown. Note the absence of PLP surface expression upon overexpression of syntaxin 3. Scale bar is 10 µm. B. Membrane microdomain association of PLP in mock-transduced and syntaxin 3-overexpressing OLGs. mOLGs (7 days differentiation) were extracted with 1% TX-100 or 20 mM CHAPS at 4°C, and analyzed by OptiPrep density gradient centrifugation. PLP was visualized by Western blotting (4C2). Detergent-resistant membrane microdomains are present in fractions 3 and 4. The blots are

representative of three independent experiments. Note that PLP is TX-100-resistant in syntaxin 3-overexpressing OLGs, whereas in mock-transduced OLGs, PLP is largely TX-100-soluble. In addition, upon overexpression of syntaxin 3, an increased fraction of PLP is CHAPS-soluble. C. ImOLGs (3 days of differentiation) were pulse-labeled with Tran35S for 10 min, which was followed by an incubation in chase medium for the indicated time intervals. Subsequently, the cells were extracted with 1% TX-100. Soluble (S, supernatant) and insoluble (I, pellet) fractions were obtained by centrifugation, after extracting equal protein amounts of total cell lysates. PLP was immunoprecipitated and the amount in the soluble and insoluble fraction was analyzed by radioactive counting. Black bars represent soluble protein and white bars represent insoluble protein. Statistical significance between 0 min and the indicated time points is shown (** $p<0.01$, *** $p<0.001$, one-way ANOVA with Tukey's post-test). Note that following biosynthesis, PLP is transiently TX-100-resistant. D. Cell surface proteins of mOLGs (10 days differentiation) were biotinylated, lysed and subjected to TX-100 extraction and OptiPrep density gradient centrifugation. Surface-localized proteins, and non-biotinylated, i.e., intracellulary-localized proteins were separated by immunoprecipitation using SA-agarose beads. PLP was visualized by Western blotting (4C2). Note, that TX-100-resistant PLP is present at the surface in membrane microdomains (fraction 4). E. imOLGs were subjected to an in situ detergent extraction with either TX-100 or CHAPS prior to fixation. Representative pictures of three independent experiments are shown. Note that TX-100-resistant PLP localized to the cell body plasma membrane, whereas CHAPS-resistant PLP mainly resided intracellularly. Scale bar is 10 μm.

3.3. Following biosynthesis, PLP transiently associates with TX-100-resistant microdomains

To obtain further support and mechanistic insight into the potential involvement of a transcytotic mechanism, underlying myelin-directed trafficking of PLP, we next examined PLP dynamics by characterizing its lateral membrane organization, applying detergent insolubility as a criterion. It has been well-documented that upon myelin biogenesis, PLP ultimately integrates into CHAPS-resistant membrane microdomains [10,39]. Given the apical-like nature of trafficking directed towards the cell body plasma membrane in OLGs, the observed inhibition of PLP transport to the surface upon overexpression of syntaxin 3 therefore suggests an inhibition of an apical-directed transport step for PLP. In general, apical protein transport is often associated with the protein's integration into TX-100-resistant membrane microdomains [40]. To verify this hypothesis in case of PLP transport, syntaxin 3-overexpressing OPCs were allowed to differentiate into myelin-like membrane forming mature OLGs, extracted with either CHAPS or TX-100, loaded on an OptiPrep density gradient and analyzed by Western blot. Whereas in control, mock-transduced cells PLP essentially localizes to TX-100-soluble but CHAPS-insoluble fractions (Fig. 2B, mock, TX-100 and CHAPS, fractions 3 and 4), in syntaxin 3-overexpressing cells PLP is largely recovered in the TX-100-insoluble fraction and much less so (approx. 50%) in the CHAPS-insoluble fraction (Fig. 2B, S3↑, TX-100 and CHAPS, fractions 3 and 4). Thus, these data would suggest that PLP, following its biosynthesis, transiently integrates into TX-100-resistant microdomains, reflecting the apical-like plasma membrane-directed transport

mechanism, which precedes a subsequent relocalization and transport step involved in its ultimate deposition at myelin-like membranes, which relies and depends, respectively, on a CHAPS-insoluble membrane localization (c.f.[10]).

To verify this potential scenario further, we next carried out a pulse-chase experiment to better define the initial steps in PLP trafficking. OLGs were metabolically labeled with Tran35S for 10 min at 37°C. Subsequently, excess non-radioactive methionine was added, and the cells were chased for 0, 15, 30 and 60 min, followed by extraction with 1% TX-100 and analysis of radiolabeled PLP in pellet (insoluble) and supernatant (soluble). As shown in Fig. 2C, during the first 15 min following de novo biosynthesis of PLP, essentially the entire PLP fraction was present within a TX-100-resistant fraction (white bars), while over the next 45 min, PLP gradually partitioned in a TX-100-soluble fraction (black bars). These data further support the notion that de novo synthesized PLP is initially assembled into TX-100-insoluble membrane microdomains, localized within transport vesicles that presumably dock in a syntaxin 3-dependent mechanism at the plasma membrane. The subsequent disappearance of PLP from such domains, as seen to gradually occur over the next 15-60 min (Fig. 2C), suggests a dynamic behavior of PLP, possibly effectuated once arriving at the cell surface of the plasma membrane.

To determine whether TX-100-resistant PLP-containing membrane fractions are in fact present at the cell surface, mature OLGs were surface biotinylated, followed by TX-100 extraction and analysis by OptiPrep density gradient fractionation. To separate surface localized (i.e., biotinylated) TX-100-resistant PLP from intracellular (i.e., non-biotinylated) TX-100-resistant PLP, the gradient fractions were next subjected to streptavidin precipitation, and analyzed by Western blot. As shown in Fig. 2D, PLP was present at the surface and this surface pool partitioned roughly equally between a TX-100-resistant (fractions 3 and 4) and TX-100-soluble fraction (fractions 6 and 7). Of the intracellular fraction, less than 15% was resistant to solubilization by TX-100. As this biochemical characterization does not provide information on the actual (surface) membrane localization of PLP, i.e., cell body plasma membrane versus myelin-like membrane, we next visualized PLP in TX-100-resistant membrane domains by an in situ extraction with TX-100 prior to fixation. TX-100-resistant PLP was mainly observed in the cell body plasma membrane (Fig. 2E, TX-100). In contrast, CHAPS-resistant PLP mainly resides intracellularly (fig. 2E, CHAPS). Hence, these findings are consistent with the notion that PLP is transported to the cell body plasma membrane, prior to myelin-like membranes. During this early processing, the protein appears to reside transiently in membrane microdomains at the cell body plasma membrane that are TX-100-resistant. The prominent intracellular CHAPS-resistance of PLP then presumably reflects the ensuing transport vesicle-mediated processing of the protein

from the plasma membrane towards the myelin membrane. To obtain further support for the ability of PLP to engage ina transcytotic transport route, we next analyzed PLP transport in the well-polarized hepatic cell line HepG2.

3.4. PLP is present at apical and basolateral domains in polarized HepG2 cells

Polarized HepG2 cells display two structurally and functionally different plasma membrane domains (Fig. 3A). The two membrane domains are separated by tight junctions and comprise the apical membrane that faces the bile canaliculus (BC), and the basolateral domain which faces adjacent cells. In these cells, direct routes for basolateral and apical delivery exist as well as indirect transcytotic routes [41]. More specifically, in previous work [36] we have provided evidence that in these cells resident apical proteins may employ different pathways to reach the apical surface following biosynthesis. Thus, whereas single transmembrane proteins traffic to the apical membrane via the basolateral membrane, thus exploiting an indirect transcytotic pathway, multispanning membrane proteins may arrive at the apical surface along a direct pathway, after exiting the Golgi. To define polarized transport properties of the multimembrane spanning PLP in these cells, we transfected HepG2 cells with PLP-eGFP. In stably transfected cells, PLP-eGFP was prominently present at the apical (BC) surface (Fig. 3B, arrow), whereas a fraction was also detectable at the basolateral surface (Fig.3B, arrowhead). Surprisingly, the PLP-eGFP at the basolateral membrane, was not recognized by the anti-PLP O10 antibody (data not shown), implying an inaccessibility of PLP's conformational epitope in HepG2 cells. However, the anti-PLP ET3 antibody does recognize extracellular PLP-eGFP at the basolateral surface (Fig. 3C). To examine whether PLP's detergent (in)solubility resembles its (in) solubility in OLGs, HepG2-PLP-eGFP cells were subsequently extracted with either TX-100 or CHAPS, followed by OptiPrep density gradient centrifugation and Western blot analysis. As shown in Fig.3D, at steady state conditions, PLP-eGFP primarily associated with CHAPS-insoluble membrane microdomains, whereas only a minor fraction was TX-100-insoluble. Thus, at these conditions PLP-eGFP partitioned in microdomains, displaying similar detergent resistance properties as in primary OLGs (cf. Fig. 2B, mock). In situ extraction revealed that CHAPS-resistant PLP is present at both the apical and basolateral membrane, whereas the PLP fraction that resisted TX-100 extraction was exclusively associated with the apical domain (Fig. 3E). Quantitative analysis, based upon the use of MRP2 as a TX-100- and CHAPS-resistant apical marker, revealed that upon in situ extraction with TX-100, only 5-10% of the MRP2-postive apical membranes are positive for PLP-eGFP, whereas upon in situ extraction with CHAPS, 60-70% of the apical membranes are positive for PLP (Fig.

3F). In control cells, approx. 85% of the MRP2-positive apical membranes are positive for PLP-eGFP. Therefore, these findings show that in HepG2 cells PLP was associated with TX-100-resistant microdomains, which were present at the apical, but not basolateral membrane, whereas CHAPS-resistant PLP resided at both membranes. Since PLP localized at both surfaces, albeit to different extents, it was of obvious interest to better define its transport itinerary. Thus, to verify whether PLP-eGFP, as a multispanning membrane protein, is transported in a direct manner to the apical surface or, alternatively, may employ an indirect transcytotic pathway from the basolateral to the apical surface, an antibody-trafficking assay was performed, as described previously [36]. HepG2-PLP-eGFP cells were incubated for 30 min (on ice) with anti-extracellular PLP ET3 antibody, followed by a 90 min incubation at 37°C to activate trafficking, and subsequent immunocytochemical analysis of the localization of the antibody-antigen complex. As shown in Fig. 3G, the antibody-stained PLP-eGFP became internalized, but did not reach the apical membrane following an incubation period of 60 min. In contrast, DPPIV, a single pass resident apical membrane protein and a marker for basolateral to apical transcytosis in HepG2 cells [36], is transported to the apical domain upon antibody internalization over the same incubation period at 37°C (Fig. 3G), indicating that basolateral to apical transcytosis is functional in the HepG2 cells that express PLP-eGFP. Therefore, these findings suggest that PLP, as a multispanning membrane protein, is directly and effectively transported to the apical membrane in polarized HepG2 cells, following biosynthesis. Subsequently, PLP may engage in transcytotic transport to the basolateral surface, where re-internalization may occur without ensuing effective re-delivery of PLP to the apical surface.

To obtain further insight into the underlying mechanism that drives polarized PLP transport, we focused on the potential role of glycosphingolipids, prompted by the transient localization of PLP in distinct membrane microdomains, as occurs in both OLGs and HepG2 cells. GalC and sulfatide are major galactolipids typically enriched in myelin, their expression preceding the appearance of PLP in OLGs [2]. Participation of both galactolipids in PLP transport has been suggested, although the role of sulfatide is still a matter of controversy. Whereas GalC and sulfatide are highly enriched in OLGs, but not in HepG2 cells, we next analyzed the expression of GalC and sulfatide in PLP-eGFP expressing HepG2 cells. As shown in Fig. 3H, upon stable expression of PLP-eGFP, the expression of sulfatide was dramatically increased as compared to parental cells (approx. 2-fold), suggesting a potential link between PLP and sulfatide expression. Hence, upon stable expression of PLP, HepG2 cells likely adapt by increasing the levels of sulfatide. This finding is rather surprising, given a reported role for GalC-enriched microdomains, but not sulfatide in PLP transport to the myelin-like membranes [10]. However, although controversial, sulfatide has been implicated in PLP transport

[42,43]. The apparent contradictory findings likely originate from the different experimental conditions, among others the polarized status of the cells. Therefore, we next revisited the role of sulfatide in PLP transport in OLGs.

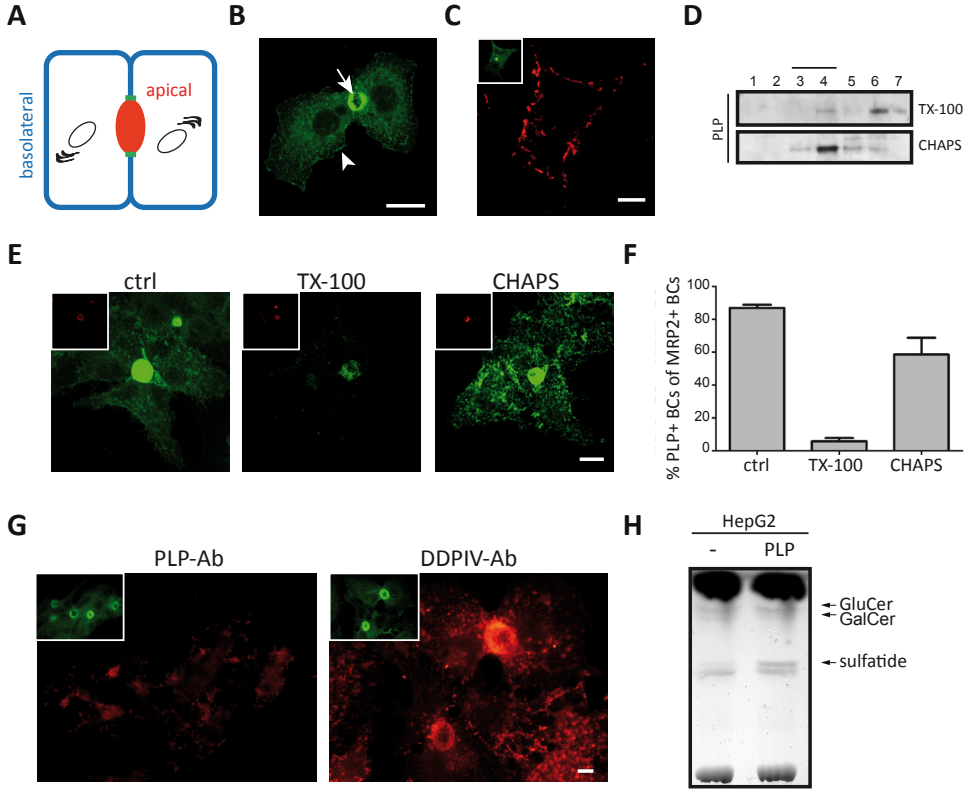

Figure 3. PLP-eGFP is present at apical and basolateral membrane domain in polarized HepG2 cells.

A. Schematic model of polarized HepG2 cells. The apical (bile canaliculus (BC), red) and basolateral (blue) membrane domains are separated by tight junctions (green). B. Localization of PLP-eGFP upon stable expression in HepG2 cells. Note that PLP-eGFP is present at the apical (arrow) and basolateral (arrowhead) membrane domain. Scale bar is 10 µm. C. Localization of extracellular PLP (ET3 antibody) and total PLP-eGFP (inset) at the basolateral surface upon stable expression in HepG2 cells. Scale bar is 10 µm. D. Membrane microdomain association of PLP-eGFP in HepG2 cells. HepG2-PLP-eGFP cells were extracted with 1% TX-100 or 20 mM CHAPS at 4°C, and analyzed by OptiPrep density gradient centrifugation. PLP-eGFP was visualized by Western blotting (anti-GFP antibody). Detergent-resistant membrane microdomains are present in fractions 3 and 4. The blots are representative of three independent experiments. E. HepG2-PLP-eGFP cells were untreated (ctrl) or subjected to an in situ detergent extraction with either 1% TX-100 or 20 mM CHAPS prior to fixation. The localization of apical membranes was visualized by immunostaining for the apical marker MRP2 (insets, red). Representative pictures of three independent experiments are shown. Note that TX-100-resistant PLP-eGFP (green) localized to some of the apical membranes, whereas CHAPS-resistant PLP-eGFP (green) resided at both membrane domains and intracellular. Scale bar is 10 µm. F. The number of PLP-positive of total MRP2-positive BCs

was determined at the indicated conditions. Each bar represents the mean + SD of three independent experiments. G. Basolateral to apical transcytosis of PLP-eGFP and DPPIV as analysed by an antibody trafficking assay. HepG2-PLP-eGFP cells were incubated for 30 min at 4°C with anti-PLP (ET3) or anti-DPPIV, after which internalization was allowed for 90 min at 37°C. Antibodies (red) were visualized by immunostaining. Note that DPPIV, but not PLP-eGFP, was transcytosed to the apical membrane domain (BC) upon antibody internalization. The localization of total PLP-eGFP is shown in the insets (green) Scale bar is 10 µm. H. TLC analysis of cellular glycosphingolipids in HepG2 and HepG2-PLP-eGFP cells. Note that the expression of sulfatide is increased upon stable transfection of PLP-eGFP.

3.5. Sulfatide is not essential for the transport of PLP to the cell body plasma membrane

Previously, we have shown that GalC and sulfatide are differently distributed in mature OLGs, GalC preferentially localizing to myelin-like membranes and compact myelin, whereas sulfatide is largely excluded from myelin-like membranes and enriched in paranodes [44]. Co-labeling of PLP and either GalC or sulfatide in fixed and permeablized mature OLGs showed that intracellular PLP and GalC co-localize (Supp. Fig. 1), whereas sulfatide is mainly present at the plasma membrane of the cell body and processes and hardly co-localized with intracellular PLP. To assess whether sulfatide is a priori involved in mediating transport of PLP, we next examined the cellular localization of PLP in primary immature OLGs, i.e., conditions at which PLP transport to the cell body plasma membrane is already apparent (c.f. Fig. 1A), upon inhibition of sulfatide biosynthesis using sodium chlorate from OPCs onwards. Sodium chlorate is a competitive inhibitor of sulfation, thus inhibiting sulfatide biosynthesis, but not that of GalC [45–47]. Labeling of cell surface PLP, with antibody ET3 in live cells, followed by fixation, permeabilisation and staining of PLP with 4C2 [29], revealed that in cells in which sulfatide biosynthesis was blocked, PLP localized predominantly at the plasma membrane of the cell body, whereas in control cells, PLP was mainly localized intracellularly (Fig. 4A). A quantitative analysis of the cells showing cell surface staining revealed a 3-fold increase in PLP surface staining upon inhibition of sulfatide biosynthesis, compared to control cells (Fig. 4B). In conjunction with a reduced intracellular staining of PLP (Fig. 4A), the accumulated surface fraction of PLP presumably reflects a decrease in PLP internalization by the cells. Remarkably, irrespective of sulfatide inhibition, PLP expressed on the surface of immature OLGs does not yet expose the O10 epitope (Fig. 4B), indicating that along its transport pathway PLP is subjected to conformational alterations. Nevertheless, sulfatide is not essential for PLP transport to the membrane surface of the cell body, given the presence of PLP at the surface upon sulfatide depletion (Fig. 4A and B).

To further confirm that sulfatide is not essential for PLP transport to the plasma membrane, PLP surface expression was visualized by anti-PLP ET3 antibody staining

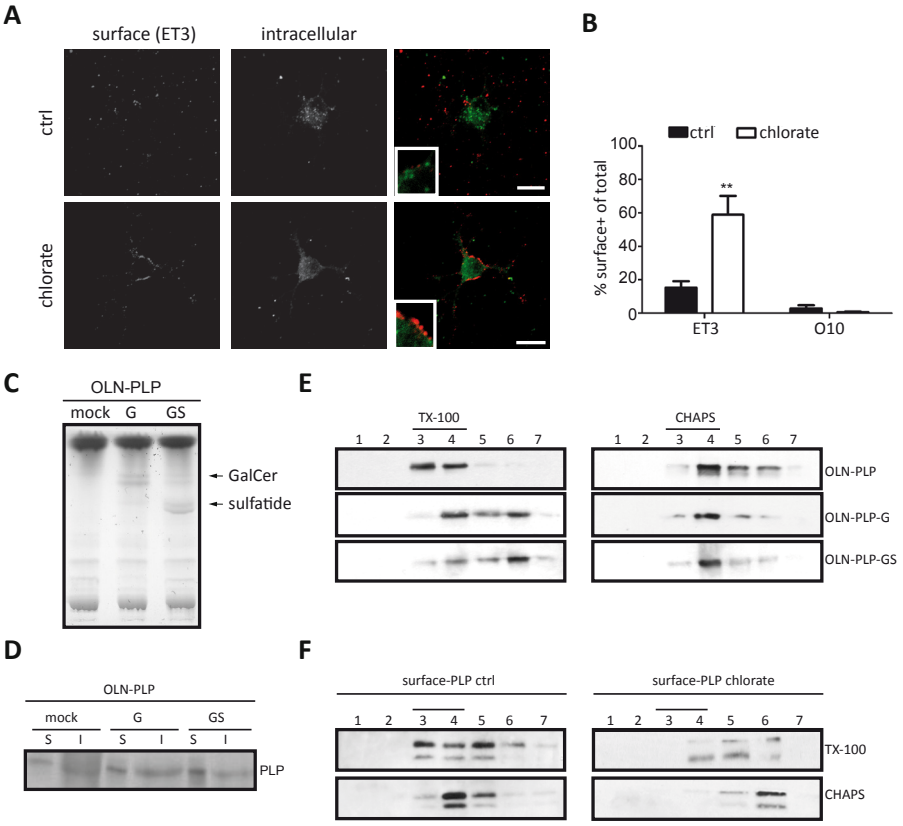

Figure 4. Sulfatide is essential for segregation to TX-100 soluble membrane microdomains.
A, B. Oligodendrocyte progenitor cells were differentiated for 3 days in the absence (ctrl) or presence of 30 µM sodium chlorate, an inhibitor of sulfatide synthesis. The surface localization of PLP was determined by immunostaining of live cells using anti-PLP antibodies directed against extracellular (ET3, O10), followed by fixation, opening and staining with the anti-PLP-4C2 antibody. Representative pictures of three independent experiments (A) and the % of surface-positive cells (B) are shown. Statistical differences with control cells (ctrl) as assessed with a student t-test (** $p< 0.001$). Note the prominent PLP surface expression at the cell body plasma membrane upon inhibition of sulfatide biosynthesis. Scale bar is 10 µm. C. TLC analysis of cellular glycosphingolipids in OLN-PLP (mock), OLN-PLP-G (GalC) and OLN-PLP-GS (GalC and sulfatide) cells. D. Cell surface proteins were biotinylated, lysed and immunoprecipitated with SA-agarose beads, to separate surface-localized proteins (s), and non-biotinylated, i.e., intracellulary-localized (i) proteins. PLP-eGFP was visualized by Western blotting (anti-GFP antibody). Note that PLP-eGFP is present at the cell surface of OLN-PLP cells (mock), i.e., in the absence of GalC (G) and sulfatide (S). E. OLN-PLP, OLN-PLP-G and OLN-PLP-GS cells cultured for 3 days in DMEM and 0.5% FCS were extracted with 1% TX-100 or 20 mM CHAPS at 4°C, and analyzed by OptiPrep density gradient centrifugation. PLP-eGFP was visualized by Western blotting (anti-GFP antibody). Detergent-resistant membrane microdomains are present in fractions 3 and 4. The blots are representative of three independent experiments. Note that PLP-eGFP is TX-100-resistant in the absence of sulfatide. F. Oligodendrocyte progenitor cells were differentiated for 7 days in the absence (ctrl) or presence of 30 µM sodium chlorate. Cell surface proteins of mature OLGs (7 days in differentiation) were biotinylated, lysed and subjected to either 1% TX-100 or 20 mM CHAPS extraction and OptiPrep density gradient centrifugation. Surface-localized proteins were immunoprecipitated using SA-agarose beads,

and surface PLP was visualized by Western blotting (4C2 antibody). Note that surface PLP is TX-100- and CHAPS-resistant in control cells,whereas upon inhibition of sulfatide synthesis (chlorate), surface PLP is CHAPS-soluble.

in an oligodendroglial derived cell line, OLN-93, expressing PLP-eGFP, but not GalC and sulfatide (Fig. 4C, mock). As shown in Supp. Fig.2, PLP-eGFP was prominently expressed at the surface of OLN-PLP cells (mock), corroborating that GalC and sulfatide were not required for transport to the plasma membrane. Surface biotinylation experiments confirmed the plasma membrane localization of PLP-eGFP in galactolipid-deficient OLN-PLP cells (Fig. 4D, mock, surface (s) vs intracellular (i)). Importantly, as in primary OLGs, overexpression of syntaxin 3 dramatically reduced the surface levels of PLP in OLN-PLP cells (Supp. Fig. 2, S3↑, arrow), suggesting a similarity in underlying mechanism in plasma membrane directed transport in both cell types. Therefore, these findings are consistent with previous findings that sulfatide is not essential for the transport of PLP to the oligodendroglial plasma membrane [45,46].

3.6. Sulfatide is necessary for PLP's reallocation to TX-100-soluble membrane microdomains

To further clarify the role of GalC and sulfatide in PLP transport and its lateral membrane distribution, OLN-PLP cells were transduced with constructs that express ceramide galactosyl transferase (CGT), the enzyme catalyzing the final step in GalC biosynthesis and/or ceramide sulfatide transferase (CST), which catalyzes the biosynthesis of sulfatide. The GalC-overexpressing and GalC- and sulfatide-overexpressing OLN-PLP cells are referred to as OLN-PLP-G and OLN-PLP-GS, respectively. TLC analysis revealed that compared to mock-transduced cells (OLN-PLP, i.e., vector-only), OLN-PLP-G express significant levels of GalC, while both GalC and sulfatide are present in OLN-PLP-GS (Fig. 4C). Of interest, the presence of both galactolipids, and to a lesser extent the presence of GalC alone, resulted in an approx. 2 fold increase in surface expression of PLP-eGFP (Fig. 3D). Given that PLP partitions in either TX-100- or CHAPS-resistant membrane domains (Fig. 2), the lateral distribution of PLP-eGFP in OLN-PLP, OLN-PLP-G and OLN-PLP-GS cells was analyzed by means of TX-100 or CHAPS extraction. In OLN-PLP-GS cells, PLP-eGFP was CHAPS-resistant and TX-100-soluble, in line with PLP's resistance in primary OLGs (Fig. 2B, mock) and HepG2 cells (Fig. 3D). Strikingly, in galactolipid-deficient OLN-PLP-mock cells, PLP-eGFP is TX-100-resistant, and partly CHAPS-resistant (Fig.4E, approx. 70%), while in the sulfatide-deficient OLN-PLP-G cells, PLP-eGFP is CHAPS-resistant, and only partly TX-100-soluble (approx. 50%). In all OLN lines, PLP acquired CHAPS-resistance,

indicating that in OLN-93 cells, the presence of sulfatide is not a prerequisite for PLP's sequestration in CHAPS-resistant domains. However, the presence of sulfatide caused PLP-eGFP to redistribute into membrane microdomains that are soluble in TX-100. To examine whether sulfatide is also a determining factor for PLP to reallocate to TX-100-soluble membrane microdomains in primary OLGs, control and sodium chlorate-treated mature OLGs were surface biotinylated, after which the protein's lateral domain distribution at the plasma membrane was analysed by means of detergent extraction followed by OptiPrep gradient fractionation and Western blot analysis. The fraction of PLP present at the surface of control mature OLGs was partly TX-100-resistant and CHAPS-resistant, whereas in sodium chlorate-treated, i.e., sulfatide-depleted cells, surface PLP was still partly TX-100-resistant, but CHAPS-soluble (Fig. 4F). Thus in contrast to its role in OLN-93 cells, sulfatide is required for PLP to be sequestered into CHAPS-resistant microdomains in cultured OLGs. Accordingly, sulfatide depletion particularly results in a perturbation of CHAPS-resistant microdomains, but not TX-100-resistant domains at the cell surface. Furthermore, our data also indicate that the presence of sulfatide mediates a microdomain reallocation of PLP, as reflected by a detergent (in)solubility transition of PLP from TX-100- to CHAPS-resistance. Since PLP only transiently associates with TX-100-resistant membrane domains, i.e., upon its biosynthesis, while the protein acquires CHAPS-resistance in subsequent transcytotic transport, we next determined the location and underlying driving force of this shift in lateral membrane distribution.

3.7. Sulfatide-dependent redistribution of PLP to different microdomains at the plasma membrane

To determine whether PLP, after arrival at the plasma membrane, and sulfatide may partition within the same membrane domains at the cell surface, we first determined potential co-localization of PLP with either GalC of and/or sulfatide in live OLN-PLP-GS cells. As shown in Fig. 5A, PLP-eGFP co-localized with sulfatide (O4), but not GalC (O1) at the cell surface (see inset). In fixed and permeablized OLN-PLP-GS (Fig. 5A) and OLN-PLP-G cells (Supp. Fig. 3), intracellular PLP-eGFP co-localized with GalC, but not sulfatide, in line with observations in primary OLGs (Supp. Fig. 1). In OLN-PLP-GS cells, a patch-like appearance of intracellular sulfatide was detected (Fig. 5A), which was not observed in primary OLGs (Supp. Fig. 1). The sulfatide patches co-localized with LAMP1, but not EEA1 (data not shown, Supp. Fig. 3), and might be a reflection of a reduced ability to degrade sulfatide in OLN-PLP-GS cells. In the presence of sulfatide, an increasing PLP fraction redistributed from TX-100-insoluble to TX-100-soluble membrane domains (Fig. 4E and F).

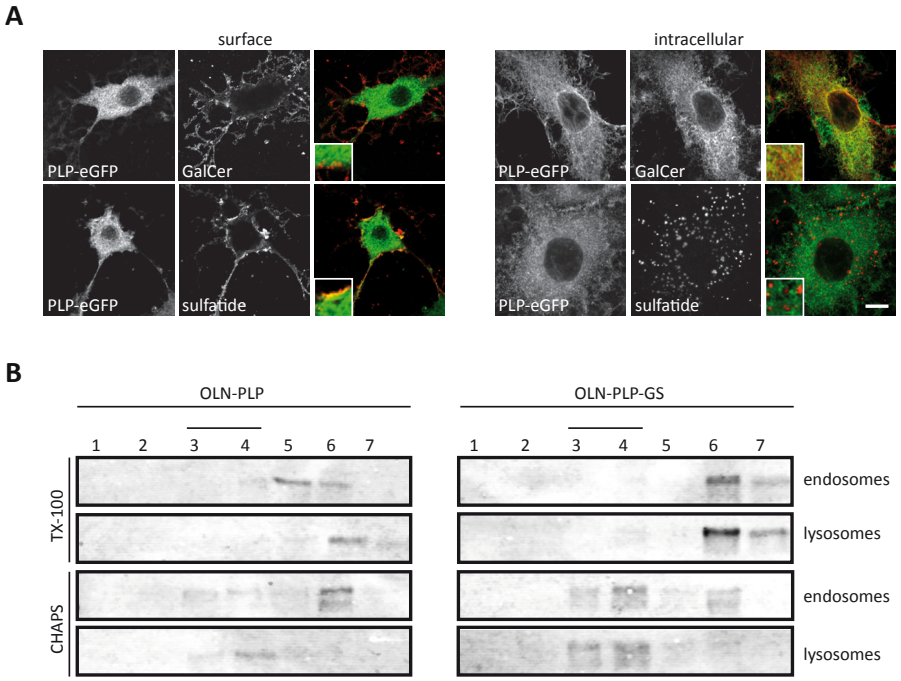

Figure 5: PLP conveys from TX-100- to CHAPS-resistant membrane microdomains at the plasma membrane.
A. Colocalization of PLP-eGFP with GalC and sulfatide in OLN-PLP-GS cells. Immunostaining with anti-GalC (O1) and anti-sulfatide (O4) antibodies was performed in live or fixed and permeabilized cells. Note that PLP-eGFP colocalized with sulfatide, but not GalC, at the surface (see inset), whereas intracellular PLP-eGFP partially colocalized with GalC, but not sulfatide (see inset).Scale bar is 10 µm. B. Enriched endosomal and lysosomal fractions of OLN-PLP and OLN-PLP-GS cells were extracted with 1% TX-100 or 20 mM CHAPS at 4°C, and analyzed by OptiPrep density gradient centrifugation. PLP-eGFP was visualized by Western blotting (anti-GFP antibody). Detergent-resistant membrane microdomains are present in fractions 3 and 4. Note that PLP-eGFP is TX-100-soluble and CHAPS-insoluble in both endosomes and lysosomes in OLN-PLP-GS cells, whereas in galactolipid-deficient OLN-PLP cells PLP-eGFP is still CHAPS-soluble in the enriched endosomal fraction.

To determine the cellular location of PLP's redistribution to TX-100-soluble membrane microdomains, i.e., at the plasma membrane or upon internalization, subcellular fractions enriched in endosomes and lysosomes were isolated, and separated on a discontinuous sucrose gradient (Supp. Fig. 4, [32,33]), followed by either TX-100 or CHAPS extraction. As shown in Fig. 5B, in OLN-PLP-GS cells, PLP-eGFP is TX-100-soluble but CHAPS-resistant in both endosomes and lysosomes, indicating that the detergent (in)solubility shift, as in HepG2-cells (Fig.3, data not shown), likely occurred at the cell surface, or immediately following internalization. In OLN-PLP cells, i.e., cells that do not express galactolipids, PLP-eGFP is CHAPS-soluble in the enriched endosomal fraction, but CHAPS-resistant in the enriched lysosomal fraction (Fig. 5B). Of note,

in OLN-PLP cells, more PLP-eGFP is present in the enriched endosomal fraction and less in the enriched lysosomal fraction as compared to OLN-PLP-GS cells (Supp. Fig. 4, fractions 3-5 vs fractions 7-8). Hence, the detergent analysis suggests that sulfatide potentially induces a lateral redistribution of PLP in the plasma membrane of OLGs, which was examined next in live cells.

3.8. Sulfatide modulates the conformation of PLP

Presumably, a change in the lateral microenvironment of a membrane protein may affect its dynamics, which, in turn, might be related to changes in the protein's structure, including oligomerization. Whether PLP could undergo such changes when sensing the presence of sulfatide at the level of the plasma membrane, we investigated this possibility by employing the three available anti-extracellular PLP antibodies in the OLN-PLP cell lines. PLP consists of four hydrophobic α-helices that span the lipid bilayer with two extracytoplasmic domains and three cytoplasmic domains, while both the C- and N terminus face the cytoplasm [27,28]. Immunocytochemical analysis in live cells revealed that the anti-PLP 4C2 antibody, which is directed against a non-conformational epitope in the first extracellular loop of PLP [29] recognizes PLP-eGFP at the surface in virtually all OLN-PLP, OLN-PLP-G and OLN-PLP-GS cells (Fig. 6A), confirming the biochemical analysis (cf. Fig. 4D) that PLP reaches the surface, independent of the presence of sulfatide. Similarly, when applying the anti-PLP ET3 antibody that recognizes a conformational epitope in the second extracellular loop, a prominent surface staining in all three OLN-lines was observed (Fig. 6A). In contrast, the O10 epitope emerged in OLN-PLP-GS cells (Fig. 6A and B) but was hardly detectable in OLN-PLP and OLN-PLP-G cells, suggesting that the presence of sulfatide is sensed by PLP, which apparently adjusted its structure in terms of conformation. Importantly, it has been reported that the O10 epitope only emerges when PLP reaches a functional tertiary structure and/or oligomerizes [30], while the secondary structure of the second extracellular loop changes as a function of its environment [31]. Given that ET3 mainly recognizes PLP at the cell body plasma membrane where sulfatide is enriched [44], whereas the O10 epitope is more prominently exposed at the myelin membrane (Fig. 1B and C), it is tempting to suggest that sulfatide likely initiates structural changes in PLP upon its internalization. In addition, given that O10 does recognize PLP-eGFP at the surface of OLN-PLP-GS cells, but not HepG2 cells (see above), this finding indicates that apparently a component is lacking in HepG2 cells that is necessary to generate the O10 epitope.

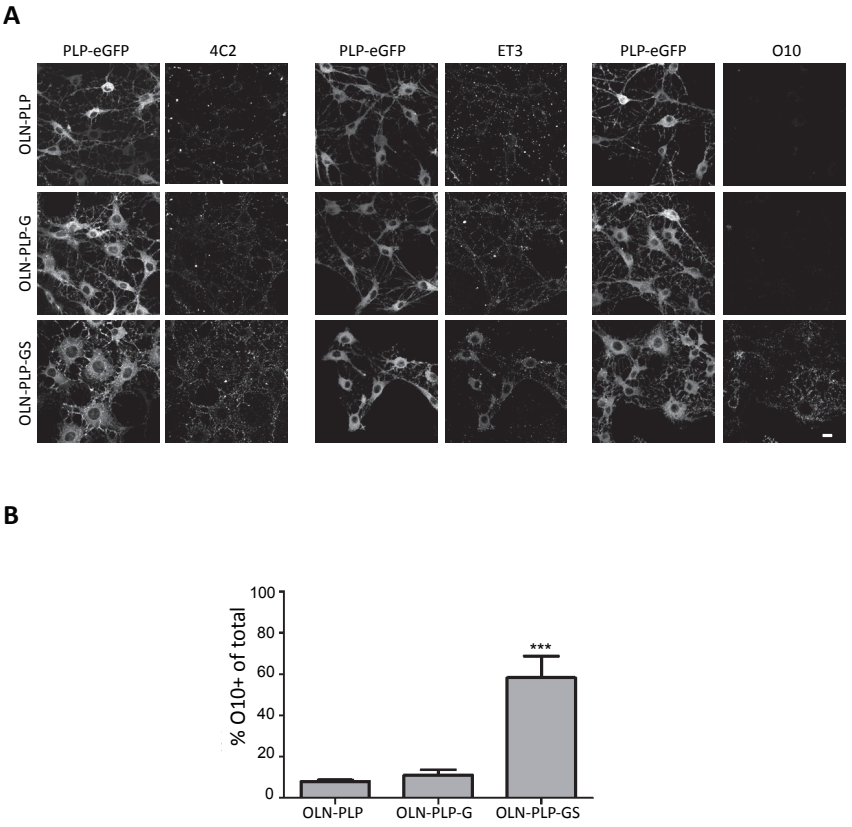

Figure 6. Sulfatide modulates the conformation of PLP at the plasma membrane.
Expression of surface PLP-eGFP in differentiated OLN-PLP, OLN-PLP-G and OLN-PLP-GS using three different anti-PLP antibodies against two distinct epitopes, i.e., the first extracellular loop (4C2) and second extracellular loop (O10, ET3) of PLP. A. Representative pictures of three independent experiments are shown. Note that O10, directed against a conformational epitope, only recognizes surface PLP-eGFP when sulfatide is present, whereas the binding of 4C2 and ET3 were not dependent on sulfatide expression. Scale bar is 10 µm. B. Quantification of the number of O10-positive cells of total cells. Each bar represents the mean + SD of at least three independent experiments. Statistical differences with OLN-PLP cells as assessed with one-way ANOVA with Tukey's post-test (*** $p < 0.001$).

4. Discussion

In the present work, we have shown that myelin biogenesis in OLGs at least partly relies on the involvement of a transcytotic transport mechanism, as reflected by myelin membrane-directed transport of PLP. Thus our data support a model in which PLP, early after biosynthesis, integrates into distinct membrane domains, characterized by TX-100 insolubility, for transport to the plasma membrane of the

OLG cell body, which relies on syntaxin 3-mediated docking (Fig. 7). At the plasma membrane, at least part of the PLP fraction is redistributed into membrane domains that are characterized by TX-100-solubility but CHAPS-resistance, consistent with previously reported observations (cf. [10]). Interestingly, inhibition of sulfatide biosynthesis in primary OLGs, and parallel experiments in OLN-93 cells, expressing GalC or GalC and sulfatide, indicate that sulfatide is instrumental in this shift in membrane domain localization, likely related to a sulfatide-induced conformational change in the protein. As shown previously, and as part of this 'apical to basolateral' transport process, PLP has become integrated in cholesterol and GalC-enriched microdomains in myelin membranes, suggesting its eventual dissociation from sulfatide [10]. Evidently, a transcytotic mechanism would be entirely in line with our previous contentions that OLGs can be envisioned aspolarized cells, displaying properties analogously to those reported for typical polarized cells like epithelial cells. In fact, in the present work we demonstrate that in such cells, i.e., hepatocytes, the major epithelial cell in the liver, PLP transcytotic transport may occur between the apical and basolateral surface.

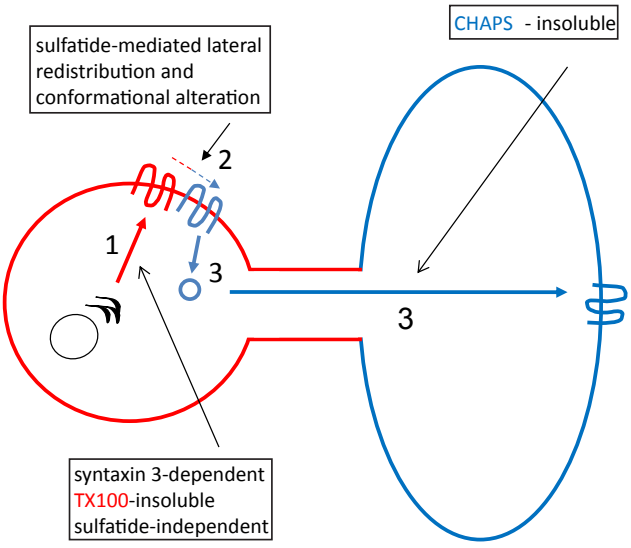

Figure 7. Schematic overview of the trafficking of de novo synthesized PLP to myelin-like membranes via transcytosis.
1. Transport of PLP from the trans-Golgi-network to the apical-like (red) plasma membrane of the cell body is syntaxin 3-dependent, sulfatide-independent and occurs as part of TX-100-insoluble, CHAPS-soluble membrane microdomains. 2. At the plasma membrane PLP is redistributed to TX-100-soluble, CHAPS-insoluble microdomains, a process that is sulfatide-mediated, and likely involves a conformational alteration. 3. Transport from the plasma membrane of the cell body to the basolateral-like (blue) myelin-like membranes occurs by means of TX-100-soluble, CHAPS-insoluble microdomains. Along this route, PLP likely temporally accumulates in a late endosomal compartment [10,11]. See text for further details.

Our observations indicate that transport of PLP to the myelin membrane relies on a syntaxin 3-dependent mechanism. Thus, following biosynthesis, PLP is first transported to the apical-like plasma membrane of the cell body in a syntaxin 3-dependent manner, after which the protein is laterally reallocated, internalized and directed towards the myelin membrane. A transient localization of PLP at the apical-like cell body plasma membrane followed by its subsequent internalization via endocytosis would, as a matter of mechanistic principle, also be consistent with observations, reported by others [15,17]. Although syntaxin 3 is clearly involved in the delivery of PLP at the cell body plasma membrane following biosynthesis, the t-SNARE involved in docking of PLP at the myelin membrane remains to be determined. Our recent data indicate that PLP transport is independent of syntaxin 4 (Bijlard et al., submitted), a typical t-SNARE that localizes at the basolateral surface in polarized epithelial cells [25] and at the basolateral-like myelin membrane [5]. The latter would thus imply the potential involvement of another transport/docking mechanism at the myelin sheet in PLP transport from the cell body plasma membrane to basolateral-like myelin membranes. A possible candidate is syntaxin 2, which like syntaxin 4 is present in OLGs and also localizes to myelin-like membranes (our unpublished observations, [21]).

At first glance our data are inconsistent with the studies of Feldmann et al. [18]. These authors proposed that vesicular delivery of PLP from endosomal compartments to the myelin membrane relies on VAMP7, the cognate v-SNARE partner of syntaxin 3, whereas our findings indicate an earlier role for syntaxin 3, i.e., in the biosynthetic pathway to the plasma membrane, rather than the transcytotic pathway. However, the conclusion of Feldmann et al. [18] on the localization of VAMP7 was primarily based on studies with GFP-VAMP7 constructs in mouse-derived Oli-neu cells that express sulfatide [48], whereas our data are derived from mature rat OLGs. Based on the current findings, it would be of interest to determine the nature of the detergent sensitivity of the PLP containing transport vesicles and sulfatide-dependence upon VAMP7 dysfunctioning, either by downregulation or overexpression of the v-SNARE, analogously as reported in the present study for a syntaxin 3-dependence of PLP transport. Nevertheless, myelin defects arise when interfering with VAMP7-mediated, but not VAMP3-mediated vesicular transport, which emphasizes that the cognate VAMP7/syntaxin 3 pair, but not VAMP3/syntaxin 4 pair, is essential for PLP transport to myelin membranes [18], which is entirely consistent with our observation in primary OLGs.

A hallmark of the transcytotic transport route of PLP is its transient partitioning into distinct membrane domains at different stages of its processing after de novo biosynthesis. Thus, following its biosynthesis, PLP is transported from the trans-Golgi-

network in a TX-100-insoluble membrane microdomain fraction to the cell body plasma membrane, where the protein redistributes to TX-100-soluble membrane domains, that in time become resistant toward CHAPS solubilization (Fig. 7). A similar sequential shift between distinct membrane domains, reflected by differences in detergent (in)solubility, was observed in polarized HepG2 cells. In further support of such a sequence of events and its functional consequences are observations reported by Simons et al. [10,49] that the kinetics of PLP's acquirement of TX-100-solubility appears to commensurate with those of acquiring CHAPS-insolubility. More specifically, PLP is largely CHAPS-soluble at the Golgi, and only after 30-60 min, i.e., likely the time required to reach the plasma membrane, PLP redistributes from a TX-100 insoluble (Fig. 2) to a CHAPS-insoluble domain [10]. As noted above, this detergent-sensitive shift, as we show here in OLGs and HepG2 cells, does likely take place at the apical membrane, rather than within endocytic compartments. Presumably, this lateral sorting step might be involved in the subsequent internalization and transport of PLP from the plasma membrane to endosomal compartments, instrumental in transcytosis [50] and subsequent delivery to the myelin membrane.

Our data indicate that sulfatide is presumably responsible for the lateral reallocation to distinct membrane microdomains. Thus, in primary OLGs, sulfatide, rather than GalC, conveys TX-100-solublilty to PLP, prior to its integration into CHAPS-resistant domains, a finding that is consistent with observations in mice that are unable to synthesize GalC and sulfatide. In these mice, a major fraction of PLP resides in TX-100 resistant domains and fails to segregate into CHAPS-resistant domains [10]. The underlying mechanism as to how sulfatide sequesters PLP from TX-100-insoluble domains remains to be determined, although sulfatide-induced conformational alterations of PLP, as reported in the present work, may be of relevance in this regard. However, of interest in this context is also the reported cholesterol-dependence of PLP's internalization before acquiring CHAPS-insolubility and the exposure of the O10 epitope [10,16]. Given that PLP and sulfatide may both associate with cholesterol [39,51], such interactions can affect the physicochemical properties of microdomains and hence their content [52]. As a consequence, sulfatide- and cholesterol-dependent invagination may be triggered, allowing subsequent transcytotic transport to the myelin membrane. Moreover, a preferential role of sulfatide in endoctytosis in OLGs has been reported [53].

Taken together, along with being a key compound in regulating the timing of terminal OLG differentiation [47,54,55], we show here that sulfatide is also a key regulator of transcytotic PLP transport, presumably relying in part on a sulfatide-induced conformational change. This may allow for a regulated timing of PLP's

appearance in myelin membranes, thereby preventing premature and ectopic compaction. Remarkably, in vivo, PLP transport to myelin membranes is uninterrupted in the absence of sulfatide [45,46,56]. Likely, under these conditions, PLP trafficking is not timely regulated and is transported to myelin membranes by bulk flow, or by an unknown compensatory, likely non-transcytotic mechanism that allows CHAPS-soluble, and possibly TX-100-insoluble PLP to insert into myelin membranes. Of interest in this context is that in the absence of sulfatide, a non-selective association with myelin-directed vesicles has been noted [57]. In addition, sulfatide interacts with several key adhesion and ECM proteins, including laminin-2 [58,59], which is secreted by developing axons [60] and promotes myelin biogenesis (reviewed in [61]). Hence, it is tempting to suggest that the recently reported interaction between laminin-2 and sulfatide in OLGs [47], might regulate (transcytotic) PLP transport in vivo, a process that may be disrupted in MS. These issues are currently investigated in our laboratory.

Acknowledgments

We gratefully acknowledge Joao Relvas for expert help in applying the retroviral expression system in oligodendrocytes, and Sven van Ijzendoorn for expert support in the HepG2 cell experiments. This work was supported by grants from the Dutch MS Research Foundation ('Stichting MS Research', WB, BK, DH), the Netherlands Organization of Scientific Research (NWO, WB, VIDI and Aspasia) and the Foundation 'Jan Kornelis de Cock'. Parts of this work was performed at the UMCG Microscopy and Imaging Center (UMIC), sponsored by NWO grant 175-010-2009-023.

References

[1] N. Baumann, D. Pham-Dinh, Biology of oligodendrocyte and myelin in the mammalian central nervous system, Physiol. Rev. 81 (2001) 871–927.

[2] S.E. Pfeiffer, A.E. Warrington, R. Bansal, The oligodendrocyte and its many cellular processes, Trends Cell Biol. 3 (1993) 191–197.

[3] H. de Vries, C. Schrage, D. Hoekstra, An apical-type trafficking pathway is present in cultured oligodendrocytes but the sphingolipid-enriched myelin membrane is the target of a basolateral-type pathway., Mol Biol Cell. 9 (1998) 599-609

[4] B. Klunder, W. Baron, C. Schrage, J. de Jonge, H. de Vries, D. Hoekstra, Sorting signals and regulation of cognate basolateral trafficking in myelin biogenesis, J. Neurosci. Res. 86 (2008) 1007–1016.

[5] W. Baron, D. Hoekstra, On the biogenesis of myelin membranes: sorting, trafficking and cell polarity, FEBS Lett. 584 (2010) 1760–1770.

[6] T. Masaki, Polarization and Myelination in Myelinating Glia, ISRN Neurology. 2012 (2012).

[7] N. Snaidero, W. Möbius, T. Czopka, L.H.P. Hekking, C. Mathisen, D. Verkleij, et al., Myelin membrane wrapping of CNS axons by PI(3,4,5)P3-dependent polarized growth at the inner tongue, Cell. 156 (2014) 277–290.

[8] V.S. Schwob, H.B. Clark, D. Agrawal, H.C. Agrawal, Electron microscopic immunocytochemical localization of myelin proteolipid protein and myelin basic protein to oligodendrocytes in rat brain during myelination, J. Neurochem. 45 (1985) 559–571.

[9] A. Gow, V.L. Friedrich Jr, R.A. Lazzarini, Intracellular transport and sorting of the oligodendrocyte transmembrane proteolipid protein, J. Neurosci. Res. 37 (1994) 563–573.

[10] M. Simons, E.M. Krämer, C. Thiele, W. Stoffel, J. Trotter, Assembly of myelin by association of proteolipid protein with cholesterol- and galactosylceramide-rich membrane domains, J. Cell Biol. 151 (2000) 143–154.

[11] E.M. Krämer, A. Schardt, K.A. Nave, Membrane traffic in myelinating oligodendrocytes, Microsc. Res. Tech. 52 (2001) 656–671.

[12] K. Ainger, D. Avossa, F. Morgan, S.J. Hill, C. Barry, E. Barbarese, et al., Transport and localization of exogenous myelin basic protein mRNA microinjected into oligodendrocytes, J. Cell Biol. 123 (1993) 431–441.

[13] L.S. Laursen, C.W. Chan, C. Ffrench-Constant, Translation of myelin basic protein mRNA in oligodendrocytes is regulated by integrin activation and hnRNP-K, J. Cell Biol. 192 (2011) 797–811.

[14] R. White, C. Gonsior, E.-M. Krämer-Albers, N. Stöhr, S. Hüttelmaier, J. Trotter, Activation of oligodendroglial Fyn kinase enhances translation of mRNAs transported in hnRNP A2-dependent RNA granules, J. Cell Biol. 181 (2008) 579–586.

[15] K. Trajkovic, A.S. Dhaunchak, J.T. Goncalves, D. Wenzel, A. Schneider, G. Bunt, et al., Neuron to glia signaling triggers myelin membrane exocytosis from endosomal storage sites, J. Cell Biol. 172 (2006) 937–948.

[16] E.-M. Krämer-Albers, K. Gehrig-Burger, C. Thiele, J. Trotter, K.-A. Nave, Perturbed interactions of mutant proteolipid protein/DM20 with cholesterol and lipid rafts in oligodendroglia: implications for dysmyelination in spastic paraplegia, J. Neurosci. 26 (2006) 11743–11752.

[17] C. Winterstein, J. Trotter, E.-M. Krämer-Albers, Distinct endocytic recycling of myelin proteins promotes oligodendroglial membrane remodeling, J. Cell. Sci. 121 (2008) 834–842.

[18] A. Feldmann, J. Amphornrat, M. Schönherr, C. Winterstein, W. Möbius, T. Ruhwedel, et al., Transport of the major myelin proteolipid protein is directed by VAMP3 and VAMP7, J. Neurosci. 31 (2011) 5659–5672..

[19] J.F. Kroepfl, M.V. Gardinier, Mutually exclusive apicobasolateral sorting of two oligodendroglial membrane proteins, proteolipid protein and myelin/oligodendrocyte glycoprotein, in Madin-Darby canine kidney cells, J. Neurosci. Res. 66 (2001) 1140–1148.

[20] D.L. Madison, W.H. Krueger, D. Cheng, B.D. Trapp, S.E. Pfeiffer, SNARE complex proteins, including the cognate pair VAMP-2 and syntaxin-4, are expressed in cultured oligodendrocytes, J. Neurochem. 72 (1999) 988–998.

[21] A. Feldmann, C. Winterstein, R. White, J. Trotter, E.-M. Krämer-Albers, Comprehensive analysis of expression, subcellular localization, and cognate pairing of SNARE proteins in oligodendrocytes, J. Neurosci. Res. 87 (2009) 1760–1772.

[22] O. Maier, T. van der Heide, A.-M. van Dam, W. Baron, H. de Vries, D. Hoekstra, Alteration of the extracellular matrix interferes with raft association of neurofascin in oligodendrocytes. Potential significance for multiple sclerosis?, Mol. Cell. Neurosci. 28 (2005) 390–401.

[23] M. Bsibsi, A. Nomden, J.M. van Noort, W. Baron, Toll-like receptors 2 and 3 agonists differentially affect oligodendrocyte survival, differentiation, and myelin membrane formation, J. Neurosci. Res. 90 (2012) 388–398.

[24] C. Richter-Landsberg, M. Heinrich, OLN-93: a new permanent oligodendroglia cell line derived from primary rat brain glial cultures, J. Neurosci. Res. 45 (1996) 161–173.

[25] S.H. Low, S.J. Chapin, T. Weimbs, L.G. Kömüves, M.K. Bennett, K.E. Mostov, Differential localization of syntaxin isoforms in polarized Madin-Darby canine kidney cells, Mol. Biol. Cell. 7 (1996) 2007–2018.

[26] O. Maier, T. van der Heide, R. Johnson, H. de Vries, W. Baron, D. Hoekstra, The function of neurofascin155 in oligodendrocytes is regulated by metalloprotease-mediated cleavage and ectodomain shedding, Exp. Cell Res. 312 (2006) 500–511.

[27] T. Weimbs, W. Stoffel, Proteolipid protein (PLP) of CNS myelin: positions of free, disulfide-bonded, and fatty acid thioester-linked cysteine residues and implications for the membrane topology of PLP, Biochemistry. 31 (1992) 12289–12296.

[28] A. Gow, A. Gragerov, A. Gard, D.R. Colman, R.A. Lazzarini, Conservation of topology, but not conformation, of the proteolipid proteins of the myelin sheath, J. Neurosci. 17 (1997) 181–189.

[29] E.A. Greenfield, J. Reddy, A. Lees, C.A. Dyer, O. Koul, K. Nguyen, et al., Monoclonal antibodies to distinct regions of human myelin proteolipid protein simultaneously recognize central nervous system myelin and neurons of many vertebrate species, J. Neurosci. Res. 83 (2006) 415–431.

[30] M. Jung, I. Sommer, M. Schachner, K.A. Nave, Monoclonal antibody O10 defines a conformationally sensitive cell-surface epitope of proteolipid protein (PLP): evidence that PLP misfolding underlies dysmyelination in mutant mice, J. Neurosci. 16 (1996) 7920–7929.

[31] E. Trifilieff, Synthesis and secondary structure of loop 4 of myelin proteolipid protein: effect of a point mutation found in Pelizaeus-Merzbacher disease, J. Pept. Res. 66 (2005) 101–110.

[32] Y. Zeng, H. Cheng, X. Jiang, X. Han, Endosomes and lysosomes play distinct roles in sulfatide-induced neuroblastoma apoptosis: potential mechanisms contributing to abnormal sulfatide metabolism in related neuronal diseases, Biochem. J. 410 (2008) 81–92.

[33] M.J. Wainszelbaum, B.M. Proctor, S.E. Pontow, P.D. Stahl, M.A. Barbieri, IL4/PGE2 induction of an enlarged early endosomal compartment in mouse macrophages is Rab5-dependent, Exp. Cell Res. 312 (2006) 2238–2251.

[34] E.G. BLIGH, W.J. DYER, A rapid method of total lipid extraction and purification, Can J Biochem Physiol. 37 (1959) 911–917.

[35] I. Sommer, M. Schachner, Monoclonal antibodies (O1 to O4) to oligodendrocyte cell surfaces: an immunocytological study in the central nervous system, Dev. Biol. 83 (1981) 311–327.

[36] T.A. Slimane, G. Trugnan, S.C.D. Van IJzendoorn, D. Hoekstra, Raft-mediated trafficking of apical resident proteins occurs in both direct and transcytotic pathways in polarized hepatic cells: role of distinct lipid microdomains, Mol. Biol. Cell. 14 (2003) 611–624.

[37] S.H. Low, S.J. Chapin, C. Wimmer, S.W. Whiteheart, L.G. Kömüves, K.E. Mostov, et al., The SNARE machinery is involved in apical plasma membrane trafficking in MDCK cells, J. Cell Biol. 141 (1998) 1503–1513.

[38] H. Fujita, P.L. Tuma, C.M. Finnegan, L. Locco, A.L. Hubbard, Endogenous syntaxins 2, 3 and 4 exhibit distinct but overlapping patterns of expression at the hepatocyte plasma membrane, Biochem. J. 329 (Pt 3) (1998) 527–538.

[39] H.B. Werner, E.-M. Krämer-Albers, N. Strenzke, G. Saher, S. Tenzer, Y. Ohno-Iwashita, et al., A critical role for the cholesterol-associated proteolipids PLP and M6B in myelination of the central nervous system, Glia. 61 (2013) 567–586.

[40] U. Coskun, K. Simons, Membrane rafting: from apical sorting to phase segregation, FEBS Lett. 584 (2010) 1685–1693.

[41] T. Aït Slimane, D. Hoekstra, Sphingolipid trafficking and protein sorting in epithelial cells, FEBS Lett. 529 (2002) 54–59.

[42] J.M. Pasquini, M.M. Guarna, M.A. Besio-Moreno, M.T. Iturregui, P.I. Oteiza, E.F. Soto, Inhibition of the synthesis of glycosphingolipids affects the translocation of proteolipid protein to the myelin membrane, J. Neurosci. Res. 22 (1989) 289–296.

[43] M.C. Brown, M.B. Moreno, E.R. Bongarzone, P.D. Cohen, E.F. Soto, J.M. Pasquini, Vesicular transport of myelin proteolipid and cerebroside sulfates to the myelin membrane, Journal of Neuroscience Research. 35 (1993) 402–408.

[44] O. Maier, D. Hoekstra, W. Baron, Polarity development in oligodendrocytes: sorting and trafficking of myelin components, J. Mol. Neurosci. 35 (2008) 35–53.

[45] R. Bansal, S.E. Pfeiffer, Inhibition of protein and lipid sulfation in oligodendrocytes blocks biological responses to FGF-2 and retards cytoarchitectural maturation, but not developmental lineage progression, Dev. Biol. 162 (1994) 511–524.

[46] M.E. van der Haar, H.W. Visser, H. de Vries, D. Hoekstra, Transport of proteolipid protein to the plasma membrane does not depend on glycosphingolipid cotransport in oligodendrocyte cultures, J. Neurosci. Res. 51 (1998) 371–381.

[47] W. Baron, M. Bijlard, A. Nomden, J.C. de Jonge, C.E. Teunissen, D. Hoekstra, Sulfatide-mediated control of extracellular matrix-dependent oligodendrocyte maturation, Glia. (2014).

[48] M. Jung, E. Krämer, M. Grzenkowski, K. Tang, W. Blakemore, A. Aguzzi, et al., Lines of Murine Oligodendroglial Precursor Cells Immortalized by an Activated neu Tyrosine Kinase Show Distinct Degrees of Interaction with Axons In Vitro and In Vivo, European Journal of Neuroscience. 7 (1995) 1245–1265.

[49] M. Simons, E.-M. Kramer, P. Macchi, S. Rathke-Hartlieb, J. Trotter, K.-A. Nave, et al., Overexpression of the myelin proteolipid protein leads to accumulation of cholesterol and proteolipid protein in endosomes/lysosomes: implications for Pelizaeus-Merzbacher disease, J. Cell Biol. 157 (2002) 327–336.

[50] D. Hoekstra, D. Tyteca, S.C.D. van IJzendoorn, The subapical compartment: a traffic center in membrane polarity development, J Cell Sci. 117 (2004) 2183–2192.

[51] Z. Pernber, K. Richter, J.-E. Mansson, H. Nygren, Sulfatide with different fatty acids has unique distributions in cerebellum as imaged by time-of-flight secondary ion mass spectrometry (TOF-SIMS), Biochim. Biophys. Acta. 1771 (2007) 202–209.

[52] C. Hao, R. Sun, J. Zhang, Y. Chang, C. Niu, Behavior of sulfatide/cholesterol mixed monolayers at the air/water interface, Colloids Surf B Biointerfaces. 69 (2009) 201–206.

[53] R. Watanabe, K. Asakura, M. Rodriguez, R.E. Pagano, Internalization and sorting of plasma membrane sphingolipid analogues in differentiating oligodendrocytes, J. Neurochem. 73 (1999) 1375–1383.

[54] Y. Hirahara, R. Bansal, K. Honke, K. Ikenaka, Y. Wada, Sulfatide is a negative regulator of oligodendrocyte differentiation: development in sulfatide-null mice, Glia. 45 (2004) 269–277.

[55] R. Bansal, S. Winkler, S. Bheddah, Negative regulation of oligodendrocyte differentiation by galactosphingolipids, J. Neurosci. 19 (1999) 7913–7924.

[56] T. Coetzee, N. Fujita, J. Dupree, R. Shi, A. Blight, K. Suzuki, et al., Myelination in the absence of galactocerebroside and sulfatide: normal structure with abnormal function and regional instability, Cell. 86 (1996) 209–219.

[57] S.N. Fewou, A. Fernandes, K. Stockdale, V.P. Francone, J.L. Dupree, J. Rosenbluth, et al., Myelin protein composition is altered in mice lacking either sulfated or both sulfated and non-sulfated galactolipids, J. Neurochem. 112 (2010) 599–610.

[58] H. Colognato, P.D. Yurchenco, Form and function: the laminin family of heterotrimers, Dev. Dyn. 218 (2000) 213–234.

[59] R. Timpl, D. Tisi, J.F. Talts, Z. Andac, T. Sasaki, E. Hohenester, Structure and function of laminin LG modules, Matrix Biol. 19 (2000) 309–317.

[60] H. Colognato, W. Baron, V. Avellana-Adalid, J.B. Relvas, A. Baron-Van Evercooren, E. Georges-Labouesse, et al., CNS integrins switch growth factor signalling to promote target-dependent survival, Nat. Cell Biol. 4 (2002) 833–841.

[61] H. Colognato, I.D. Tzvetanova, Glia unglued: how signals from the extracellular matrix regulate the development of myelinating glia, Dev Neurobiol. 71 (2011) 924–955.

Supplementary Figures

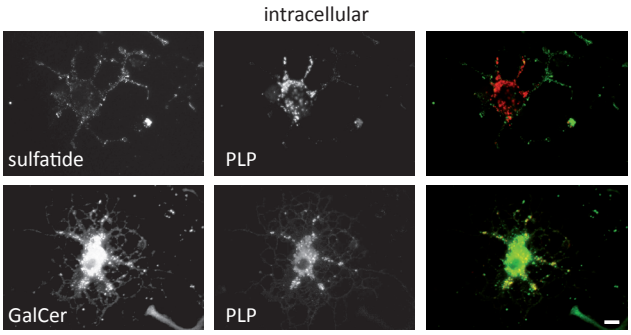

Supplementary Figure 1: Colocalization of PLP with GalC and sulfatide in oligodendrocytes. Oligodendrocytes, 7 days after initiating differentiation, were fixed, permeabilized and co-stained for PLP (red, 4C2) and galactolipids, sulfatide (green, O4 antibody) or GalC (green, O1 antibody). Representative pictures of three independent experiments are shown. Note that intracellular PLP and GalC, but not sulfatide, co-localize. Scale bar is 10 µm.

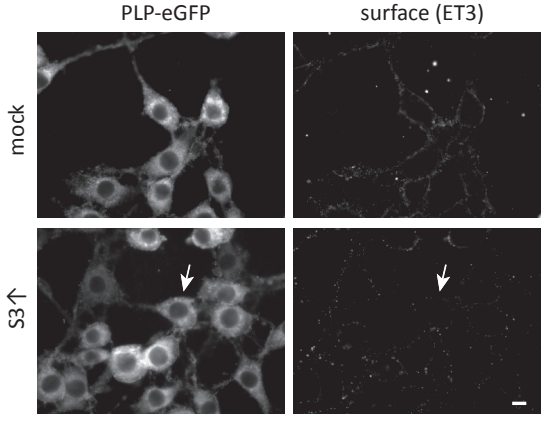

Supplementary Figure 2: Overexpression of syntaxin 3 inhibits surface transport of PLP in OLN-93 cells.
The surface localization of PLP-eGFP was determined in mock-transduced (vector only) and syntaxin 3-overexpressing cells (S3↑) in OLN-PLP cells by immunostaining using anti-PLP antibodies directed against an extracellular PLP epitope (ET3). Note decreased PLP-eGFP surface expression upon overexpression of syntaxin 3. Scale bar is 10 µm.

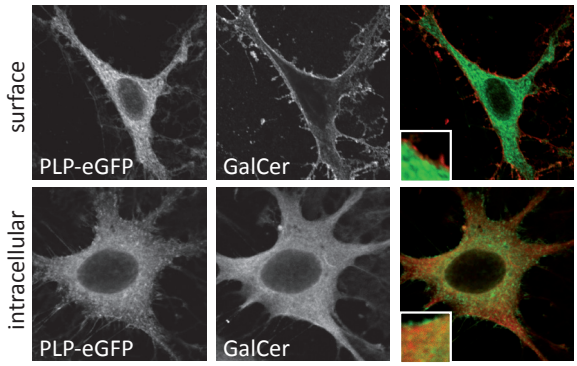

Supplementary Figure 3: Colocalization of PLP-eGFP with GalC in OLN-PLP-G cells.
Immunostaining with anti-GalC (O1) antibody was performed in live or fixed and permeabilized OLN-PLP-G cells. Note that intracellular, but not surface PLP-eGFP colocalized with GalC (see inset). Scale bar is 10 µm.

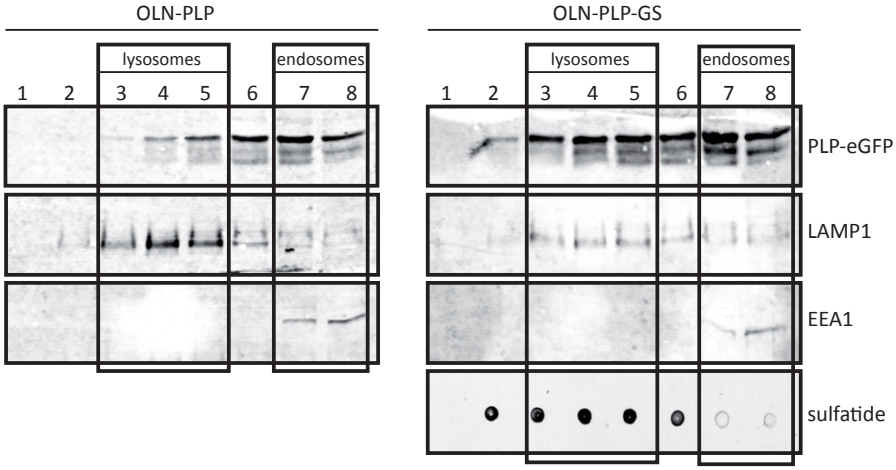

Supplementary Figure 4: Generation of fractions enriched in endosomes or lysosomes.
Organelle-fractionation and the generation of a fraction enriched in endosomes and lysosomes enriched, as marked by the expression of EEA1 and LAMP1, were obtained as described in Materials and Methods. Endosomes and lysosomes were separated from each other by a discontinuous sucrose gradient, and the distribution of EEA1, LAMP1, and PLP-eGFP (anti-GFP antibody) were visualized by Western blotting. The distribution of sulfatide is visualized with a dotblot using anti-sulfatide antibody O4 for detection. The boxes encloses the pooled fractions of the gradient used for detergent extractions of enriched endosomal and lysosomal fractions shown in Fig. 5B.